2011 IEEE International Conference on Robotics and Automation
Shanghai International Conference Center
May 9-13, 2011, Shanghai, China

Development of a Helical Climbing Modular Snake Robot

Pongsakorn Polchankajorn and Thavida Maneewarn

Abstract - **This research aims to study the grasping torque profile of the helical climbing robot on the cylindrical pole with constant radius. The modular snake robot is formed into a helical shape which can be described by various parameters such as the helical pitch angle, the radius and the pitch distance. The torque in each axis of rotation is affected by the helical pitch angle parameter. Five grasping configurations with different helical pitch angle were tested on the 18 degree of freedoms, 7 modules wheeled snake robot. The experimental result showed that the torque around yaw axis transferred to the pitch axis when the helical pitch angle was increasing. The profile of torque magnitude along the robot's body resulted in parabolic shape due to the unbalanced grasping force of the discrete points of contact between the robot and the pole.**

Keywords - Modular Snake Robot, Grasping, Pole Climbing.

I. INTRODUCTION

Snake robot, technically termed a hyper-redundant robot [1], is a mechanism that had the number of degree-of-freedoms much larger than the necessary amount required to performed the task. This type of robot consists of joints and links which have the same design can be called the modular robot. Modular robot can be divided to two types: reconfigurable and non-reconfigurable modular robot. The reconfigurable modular robot is the robot that can adapt its configuration to increase motion limitation of a chain type robot such as Conro[2], M-TRAN[3], and SUPERBOT[4]. Non-reconfigurable modular robot is the robot that restricts to its chain type form such as ACM-R3[5] and other snake robot. Most of snake robot research concern of snake-like locomotion [1, 5-8]. Some researchers were also interested in the analytical problem of inverse kinematics for a hyper-redundant robot which requires some numerical techniques to find the joint solution for a discrete approximation of a curve in three dimensional spaces.

In recent years, climbing gait of a snake robot has also became topic of interest by many researchers. Chirikjian and Burdick [1] showed an example of a grasping gait by applying the travelling wave amplitude constant (TWAC) locomotion gait to move the snake robot to coil around a cylindrical pole. Their works suggested the use of a backbone curve to solve kinematic problem in a snake robot. Andersson [6] proposed to use numerical method to solve for the joint coordinate at the universal joint snake robot in order to approximate the discretized curve. Choset[7, 8] applied the vertical helical rolling motion to the climbing gait of a snake robot. In this gait, the snake robot is formed into the helix curve configuration and rolls vertically to climb up the pole. He also suggested the concept of Toroidal Skin Drive (TSD) in which the robot skin is used for rolling laterally instead of using wheels. The TSD design was shown as driving through a small opening, crossing the gap and climbing the pole in helical trajectory. Goldman and Hong [9] analyzed the optimal design parameters for build the hyper-redundant pole climbing robot. They also present the cost function that is the main procedure of the robot. Seirei Industry [10] built the commercial pruning machine to cut tree's branches. This machine also used the helical rolling concept to climb the tree using multiple wheels that lock around the tree's trunk and roll up the tree.

Choset's works and Seirei Industry's pruning machine showed promising examples of helical pole climbing concept. This type of climbing can reduce the wheel's load compare to the direct vertical climbing. In this paper, we would like to explore the idea of a helical climbing concept in the hyper-redundant robot. We propose the different kind of helical climbing where the wheels propel the robot along the helical trajectory instead of the vertical direction. This climbing type can decrease wheel's load while climbing the pole, because of the friction that acts along the wheel axis supports some of the robot weight. Another merit of this climbing type is the stability of climbing. The helical climbing allows some difference of the wheel's velocity in each link so that the robot can maintain its shape while climbing up the pole. In this climbing gait, the wheel's load and climbing distance can be adjusted by changing a pitch of 3-D helical path. In the next section, we will discuss about the climbing gait design step. The kinematics of the proposed helical pole climbing will be explained. The parameters that affect the performance of pole climbing will be discussed and tested on our modular snake robot.

The rest of the paper is organized as follows: Section II describes how the robot climbing the pole in helical shape and in particular subsection A describes a helix path equation, while subsection B describes a frame configuration of the robot and climbing condition. Section III describes the inverse-kinematics of the snake robot, describes ratio of the weight support in each axis of the module. Section IV describes the robot's structure and a grasping experiment. Finally, discussion and conclusion are mention in section V and VI.

Manuscript received September 15, 2010. This work was supported in part by Junior Science Talent Project, NSTDA.

Pongsakorn Polchankajorn and Thavida Maneewarn are with Institute of FIeld roBOtics (FIBO), Tungkru, Bangkok 10140 Thailand; e-mail: dome @ fibo.kmutt.ac.th, praew @ fibo.kmutt.ac.th.

II. CONCEPT OF HELICAL CLIMBING

A. Circular helix path

We can use 3 equations to generate 3-D helix moving path as follow.

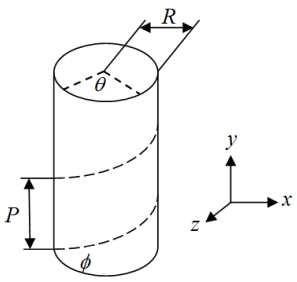

Fig. 1. Circular helix path.

$$z = R\cos(\theta) \tag{1}$$

$$x = R\sin(\theta) \tag{2}$$

$$y = \frac{P.\theta}{2\pi} = \theta R\tan\phi \tag{3}$$

Where P , R , θ , and ϕ are the pitch distance, the path's radius on xz plane (top view), the angle parameter, and the helical pitch angle.

B. Helical climb

We apply the circular helix path equations to find the position of each joint in the *n-dof* robot (origin of the *{0}* to *{n}* frame) by searching along the path for the next joint's position that has the distance from the current joint position equal to the link length of the robot. First, the tail joint is defined at the origin of frame 0. The calculation is performed iteratively for each joint until reaches the robot's head position at frame n.

After that, we use a simple algebraic solution to solve for inverse kinematics. From frame {0}, the set of joint angles (roll-pitch-yaw) that can move its next frame (frame {1}) to the correct position and orientation on the helical path with reference to its previous joint can be calculated. This operation is performed iteratively from joint *0* to *n-1*th. Dimension and reference frame in each joint which is assigned in Denavit-Hartenberg convention are shown in fig. 2.

After the robot assumes the configuration along the helical moving path, it will exert forces to the pole in order to hold its position against the gravitational force. The robot can then moves up the pole by propelling its wheel (attached on the z-axis of each module). Therefore, the robot can move along the helical path in lateral direction as long as the contact between the wheels and the pole surface provides enough friction to create a non-slipping contact.

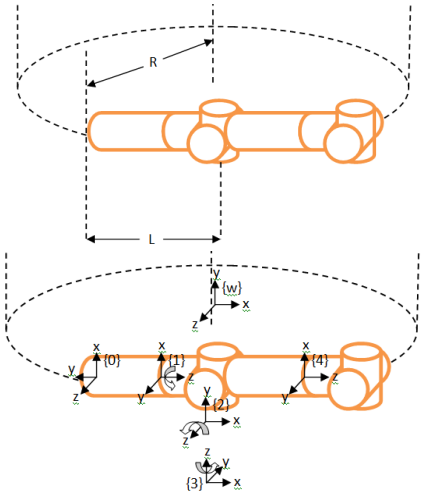

Fig. 2. Robot's frame assignment.

III. ROBOT DESIGN FOR HELICAL CLIMBING

A. Helical shape approximation

Snake robots normally require at least 2 degrees of freedom per module to fit 3-D helical curve. However we designed our robot to have 3 degrees of freedom per module because of the additional constraints that requires every wheel to contact with the pole surface for climbing.

First we define each module to have 3 dof (roll-pitch - yaw). When *i* is the number of the module, we can refer the robot's tail module at the start of the moving path as i = 0. From the 7-modules (3 dof for each joint) robot that we built for this experiment, we can refer the robot's head as i = 7. We also assign the name of each revolution axis as follows: the revolute joint that rotates around the module's x-axis is the "roll joint", the revolute joint that rotates around z-axis of the module (the axis that perpendicular to pole) is the "pitch joint", and the revolute joint that rotates around y axis of the world frame (parallel to the pole) is the "yaw joint".

After the helix path is defined, the joint location can be thought of as a discrete approximation of the helix. The rotation matrix of each link respect to world frame can be found from the relation of helical pitch angle (ϕ), circular helical radius (R), and link length (L). We can compute the rotation angle around pole axis that can align the link's frame to helical curve (θ_{step}) from the equation below.

$$\theta_{step} = 2.\text{atan2}\left(\sqrt{\frac{(s-b)(s-c)}{s(s-a)}}\right) \tag{4}$$

$$\text{Assume} \quad a = L\cos(\phi)$$

$$b = c = R$$

$$s = \frac{a+b+c}{2}$$

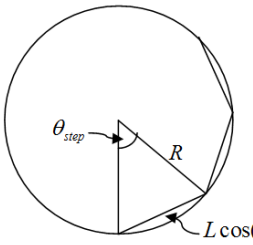

Fig. 3. Top view of the helical curve.

Then we can use θ_{step} to find the orientation of vector x, z of each link with respect to the world's frame from the equation below.

$$ {}^{w}_{z}P = \begin{bmatrix} \sin(i.\theta_{step}) \\ 0 \\ \cos(i.\theta_{step}) \end{bmatrix} \tag{5} $$

$$ {}^{w}_{x}P = \begin{bmatrix} \cos(i.\theta_{step})\cos(\phi) \\ \sin(\phi) \\ -\sin(i.\theta_{step})\cos(\phi) \end{bmatrix} \tag{6} $$

The transformed vector y with respect to world's vector y (${}^{w}_{y}P$) can be computed by the cross product of the vector ${}^{w}_{x}P$ and ${}^{w}_{z}P$. After that, we can find the rotation matrix with respect to world frame.

$$ {}^{w}_{i}R = \begin{bmatrix} {}^{w}_{x}P & {}^{w}_{y}P & {}^{w}_{z}P \end{bmatrix} \tag{7} $$

Then we can use the relation of the rotation matrix with respect to world frame to compute the rotation matrix i with respect to the frame of the link i – 1 from the equation.

$$ {}^{i-1}_{i}R = {}^{w}_{i-1}R^{T}\ {}^{w}_{i}R \tag{8} $$

So, we can find the angles that can solve for the angular solutions of the robot along the helical path in which the robot's wheels create the perpendicular contact with the pole surface by the Euler's angle set equation below. Where α , β , and γ is the roll, pitch, and yaw angle.

$$ R_{X'Z'Y'}(\alpha,\beta,\gamma) = \begin{bmatrix} c\beta c\gamma & -s\beta & c\beta s\gamma \\ c\alpha s\beta c\gamma + s\alpha s\gamma & c\alpha c\beta & c\alpha s\beta s\gamma - s\alpha c\gamma \\ s\alpha s\beta c\gamma - c\alpha s\gamma & s\alpha c\beta & s\alpha s\beta s\gamma + c\alpha c\gamma \end{bmatrix} $$

$$ {}^{i-1}_{i}R = \begin{bmatrix} m_{11} & m_{12} & m_{13} \\ m_{21} & m_{22} & m_{23} \\ m_{31} & m_{32} & m_{33} \end{bmatrix} $$

$$ = \begin{bmatrix} c\beta c\gamma & -s\beta & c\beta s\gamma \\ c\alpha s\beta c\gamma + s\alpha s\gamma & c\alpha c\beta & c\alpha s\beta s\gamma - s\alpha c\gamma \\ s\alpha s\beta c\gamma - c\alpha s\gamma & s\alpha c\beta & s\alpha s\beta s\gamma + c\alpha c\gamma \end{bmatrix} $$

$$ \alpha = \text{atan2}(m_{32}, m_{22}) \tag{9} $$

$$ \beta = a\sin(-m_{12}) \tag{10} $$

$$ \gamma = \text{atan2}(m_{13}, m_{11}) \tag{11} $$

The inverse kinematics method explained above was applied to a simulated robot and can be graphically shown in fig. 4 that it assumes the correct helical configuration.

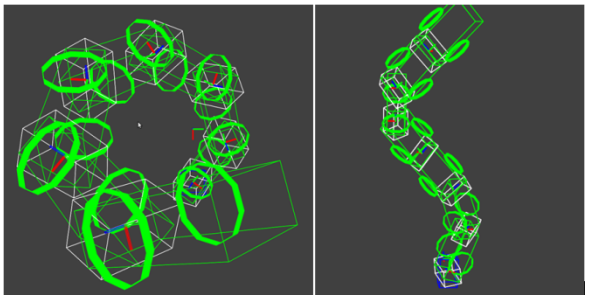
Fig. 4. The robot after apply the result angle.

B. Mechanics of helical climbing

Helical climbing of the wheel base snake robot can be divided in 2 tasks. The first task is grasping. The robot has to apply force at the contact between wheel and pole surface sufficiently to create the friction force that is larger than its weight in order to stay on the pole. The joint torque that motor applies to the contact depends on the parameters of the helix such as the pitch distance. The second task is climbing. The wheels along the robot's body have to create the rolling motion along the helical path while the three joints in each module have to maintain the robot's helical configuration and the contacts with the pole surface. The surface between wheels and pole has to allow a non-slip contact where the robot's wheel doesn't slip along the wheel axis. The wheels only roll along the helical path to propel the robot upward. Free body diagram of the robot's wheel with respect to module's frame is shown in fig. 5.

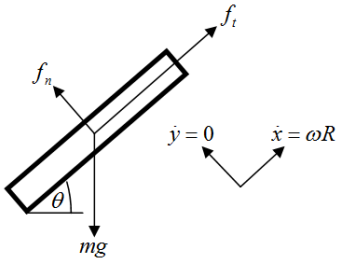

Fig. 5. Robot's wheel free body diagram.

From dynamic equation

$$ \Sigma F = ma $$

Substitute acceleration in each axis

$$ x-axis: \qquad f_t - mg\sin\phi = m(\dot{\omega}R) $$

$$ f_t = mg\sin\phi + m(\dot{\omega}R) \tag{12} $$

$$y-axis: \quad f_n - mg\cos\phi = m\ddot{x} = 0$$
$$f_n = mg\cos\phi \qquad (13)$$

Where f_n, f_t and mg are friction along wheel axis, friction along moving path, and robot's weight.

These equations show that, the larger helical pitch angle, the more torque is required to drive the robot. We can calculate ratio of weight support in each axis from eq. (12), (13). At $\phi = 45$ degrees, weight support in each axis are equal.

IV. Experiment

A. Snake robot system design

1) Mechanical design

The snake robot that we built for the experiment consists of 7 modules. The dimensions of each link are 19 cm long, 11 cm wide and 7.5 cm height. Each link connected with 3 revolute joints, which is a commercial servo (Robotis DX-117). Each link attached with 2 drive wheels. Wheel sizes are 10 cm diameter, 1 cm thickness. The wheels' surface is surrounded by Anti-slip tape. The wheel is propelled by a commercial servo (Robotis RX-28). The robot structure is made from aluminum. All joints and link are homogeneous based on modular design concept. The total weight of the robot is approximately 3 kg. The design of the robot is shown in fig. 6.

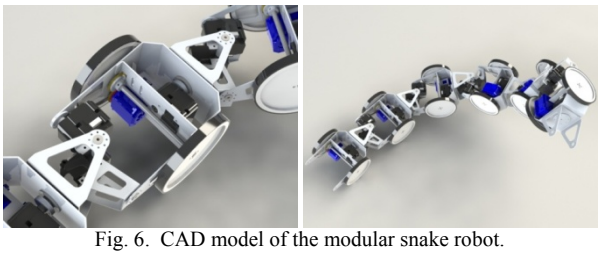

Fig. 6. CAD model of the modular snake robot.

2) Control system design

The robot's system consists of a computer, an external power supply, a microcontroller board (ATMEL ATMEGA128), and the modular snake robot. The computer, as a high level control unit, will send command such as motor's speed and angle to the microcontroller board. Then microcontroller board changes the data to the motor's protocols. These protocols are sent to all motors via RS-485. After that, position control and speed control are performed at the servo motor. The prototype robot is shown in fig. 7.

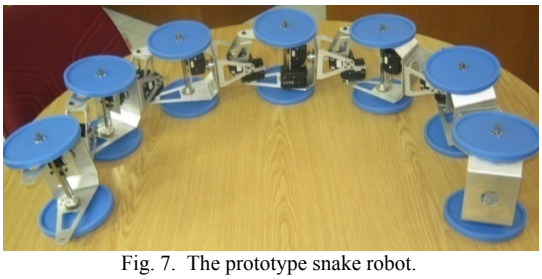

Fig. 7. The prototype snake robot.

B. Grasping result

The experiment was designed to test the performance of the circular helical grasping at various pitch distance and angle. The relation between the pitch angle and the grasping load in each motor was the main focus of this study. We tested the robot that consists of 7 modules, 14 wheels along the helical path at 15, 17.5, 20, 22.5, 25 degree pitch angle. Fig. 8 shows the image of the robot when grasping the pole at 15 and 20 degree pitch angle.

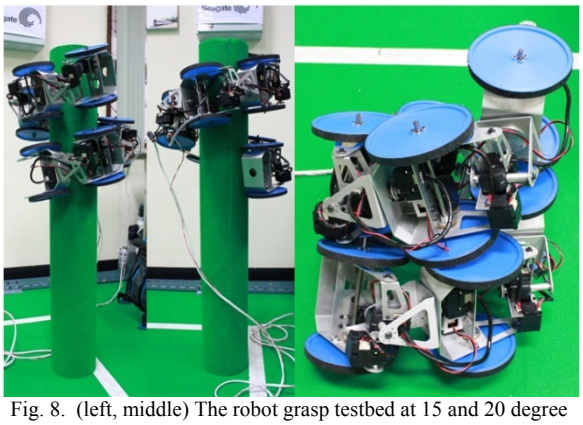

Fig. 8. (left, middle) The robot grasp testbed at 15 and 20 degree helical pitch, (right) Robot after controlled to form to helical shape.

The robot was climbing on a 14.5 cm diameter pole. An anti-slip tape was added on to the robot's wheels. The pole was wrapped with 1 mm thick carpet to create the high friction surface. Due to the wheel offset, we used 12.75 cm radius as the parameter for the helix to calculate the angle that use to control the robot in table I. The roll-pitch-yaw angles were the same for all modules because the reference frame in each module rotates and translates at the same value. At 15 degrees helical pitch angle, the robot can climb the pole at the speed of 1 m/min.

TABLE I
JOINT ANGLE USED IN THE EXPERIMENT

Helical pitch angle(degrees)	15	17.5	20	22.5	25
Roll angle	15.54	18.33	21.15	23.98	26.76
Pitch angle	-15.17	-17.02	-18.57	-19.79	-20.67
Yaw angle	88.62	85.70	82.42	78.82	74.95

We recorded the result of the torque that the robot applied to the pole by directly reading each motor's torque value via RS485. Experiment result is shown in fig. 9, fig. 10, and fig. 11.

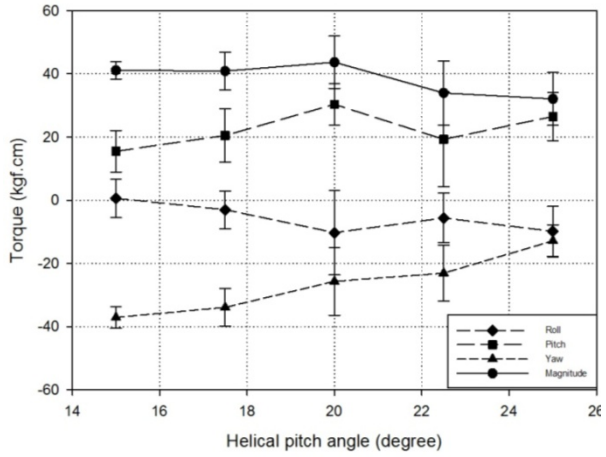

Fig. 9. The graph between mean and SD of holding torque in each axis of rotation and helical pitch angle.

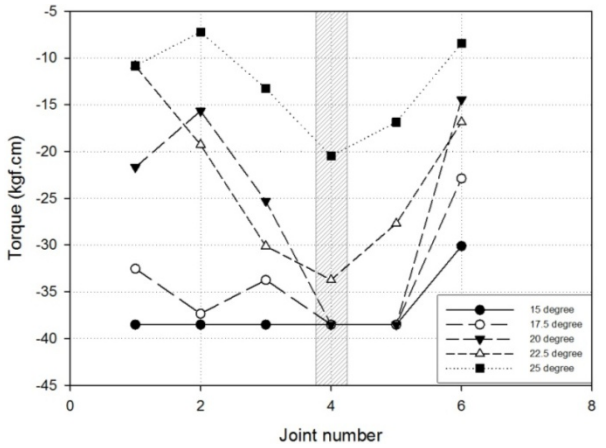

Fig. 10. The graph between holding torque of yaw angle and helical pitch angle.

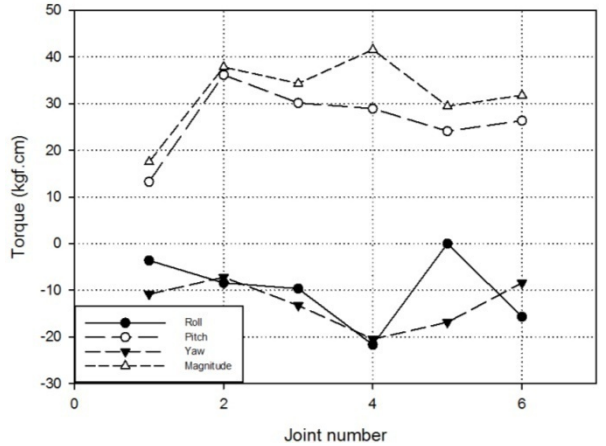

Fig. 11. The graph between holding torque and joint number at 25 degree helical pitch.

Results of the experiment in fig. 9 showed that the pitch to magnitude torque ratio and yaw to magnitude torque ratio depended on helical pitch angle. It showed that the ratio between pitch and roll torque to the total torque magnitude increased, but the ratio between the yaw torque to the total torque magnitude decreased with the larger helical pitch angle. Another two figures are also shown that the total torque magnitude, the pitch, and yaw holding torque profiles were distributed in parabolic form along the robot's body. This meant that the middle part of the robot required more power to support its neighbor module's weight and holding torque. Therefore the main factor that affects the discrepancy of torque ratio between each axis and the total torque magnitude is the helical pitch angle.

V. Discussion

After we analyzed the result of the experiment, we have found the trend of the torque in yaw axis in each helical pitch change was in parabolic shape when the robot grasped the pole. This could be the effect of grasping force from the neighbor module that acts toward the middle part of the robot more than other parts. We also calculated the resultant vector of z axis of each link in world frame that caused by the discrete point of contact between the robot and the pole. The magnitude of resultant vector is increasing when increase the helical pitch angle. The direction of resultant vector is in ranges of 178 – 180 degrees from the tail of the robot (as shown in figure 12).

TABLE II
THE TOTAL FORCE IN X AND Z AND THE RESULTANT FORCE FROM A UNIT VECTOR OF FORCE APPLYING IN EACH MODULE AT DIFFERENT HELICAL PITCH ANGLES

Helical pitch angle(degrees)	15	17.5	20	22.5	25
Force in x axis	-0.150	-0.075	-0.038	0.195	0.396
Force in z axis	-0.790	-0.913	-1.036	-1.145	-1.222
Resultant force	0.804	0.916	1.036	1.161	1.285
Resultant force direction(degree)	178.2	178.3	178.5	178.6	178.7

This range can be projected to the robot link 4-5 (as shown in gray region in fig. 10). This observation agrees with the peak of the parabolic that occurred around joint 4 in the graph between the yaw holding torque and the joint number (fig 10 and 11).

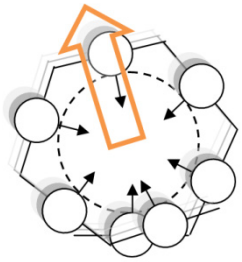

Fig. 12. Represent of resultant force.

The wheel-based hyper-redundant robot is generally easier to control in term of a climbing speed than the non-wheeled robot. In order to change the climbing speed, only the wheel velocity needs to be adjusted. However, the mechanical structure of the wheel-based robot is more complicate and it is necessary for this type of climbing that the configuration of the robot is adjusted so that the wheel of all modules are perpendicular to the climbing surface.

VI. Conclusion

In this paper, the pole climbing in helical configuration of the wheel-based modular snake robot was studied. The pole grasping was realized by forming the snake robot into a helical shape. All wheel axes of the robot need to be parallel to the pole's surface by adjusting the joint angle in each robot's module according to the inverse kinematics calculation from the predefined helix and robot's link length. Non-slip contact can be created by decrease the helical radius and increase static friction coefficient between wheels' surface and pole surface. The grasping experiment was performed to study the relationship between helical pitch angle and holding torque in each link. When the helical pitch angles increase, yaw holding torque decreases, while roll and pitch holding torque and helical pitch increase. The distribution of torque along the robot body resulted in a parabolic shape. As long as the non-slip contact is maintained, the helical pitch angle is the main factor that affects the torque requirements of the robot. In the near future, we will focus more on the climbing experiment in order to find the relationship between the drive load, the holding load, the climbing velocity and the helical pitch angle.

References

[1] Chirikjian, G. S. and Burdick, J. W., 1995, "Kinematically optimal hyper-redundant manipulator configurations." *IEEE Transactions on Robotics and Automation 11*: 794-806.

[2] A. Castano, A. Behar, P. Will, 2002, "The Conro Modules for Reconfigurable Robots", *IEEE/ASME Trans. Mechatronics*, 7(4):403–409.

[3] H. Kurokawa, K. Tomita, A. Kamimura, S. Murata, Y. Terada, S. Kokaji, 2006, "Distributed Metamorphosis Control of a Modular Robotic System M-TRAN", *Distributed Autonomous Robotic Systems (DARS) 7*, *Springer*, 115-124.

[4] B. Salemi, M. Moll, W. Shen, 2006, "SUPERBOT: A Deployable, Multi-Functional, and Modular Self-Reconfigurable Robotic System", *Proc. Intl. Conf. on Intelligent Robots and Systems*.

[5] M. Mori, S. Hirose, 2001, "Development of Active Cord Mechanism ACM-R3 with Agile 3D mobility", *Proc. Intl. Conf. on Robotics and Automation*, 1552-1557.

[6] Sean B. Andersson, 2006. "Discrete approximations to continuous curves", *IEEE International Conference on Robotics and Automation*.

[7] Kevin Lipkin, Isaac Brown, Aaron Peck, Howie Choset, Justine Rembisz, Philip Gianfortoni, Allison Naaktgeboren, 2007. "Differentiable and Piecewise Differentiable Gaits for Snake Robots", *IEEE/RSJ International Conference on Intelligent Robots and Systems.*

[8] James C. McKenna, David J. Anhalt, Frederick M. Bronson, H. Ben Brown, Michael Schwerin, Elie Shammas, and Howie Choset, 2008. "Toroidal Skin Drive for Snake Robot Locomotion", *IEEE International Conference on Robotics and Automation*.

[9] G. Goldman and D. W. Hong, 2008, "Considerations for Finding the Optimal Design Parameters for a Novel Pole Climbing Robot", *ASME Mechanisms and Robotics Conference*.

[10] Seirei industry co.,ltd, 2000, Prunning machine AB232R [Online], Available : http://www.seirei.com/products/fore/ab232r/ab232r.html# [2/11/2009].

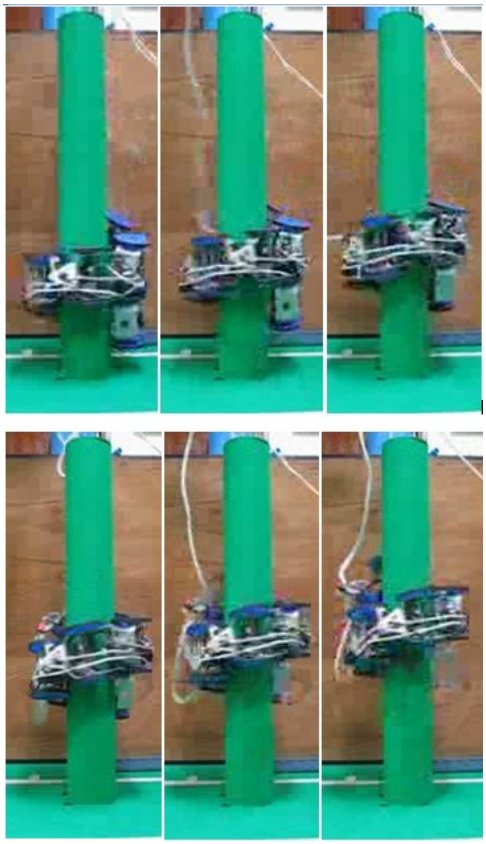

Fig. 13. Climbing experiment of the robot.